

Influences of annealing temperature on properties of Fe^{2+}:ZnSe thin films deposited by electron beam evaporation and their applications for *Q*-switched fiber laser

Du-Xin Qing(卿杜鑫), Shu-Tong Wang(王树同), Shou-Gui Ning(宁守贵), Wei Zhang(张伟), Xiao-Xu Chen(陈晓旭), Hong Zhang(张弘), Guo-Ying Feng(冯国英), Shou-Huan Zhou(周寿桓)
Citation: Chin. Phys. B . 2020, 29(5): 054208 . **doi:** 10.1088/1674-1056/ab81f2
Journal homepage: http://cpb.iphy.ac.cn; http://iopscience.iop.org/cpb

What follows is a list of articles you may be interested in

Influence of low-temperature sulfidation on the structure of ZnS thin films

Shuzhen Chen(陈书真), Ligang Song(宋力刚), Peng Zhang(张鹏), Xingzhong Cao(曹兴忠), Runsheng Yu(于润升), Baoyi Wang(王宝义), Long Wei(魏龙), Rengang Zhang(张仁刚)
Chin. Phys. B . 2019, 28(2): 024214 . **doi:** 10.1088/1674-1056/28/2/024214

Carboxyl graphene oxide solution saturable absorber for femtosecond mode-locked erbium-doped fiber laser

Rui-dong Lv(吕瑞东), Lu Li(李璐), Yong-gang Wang(王勇刚), Zhen-dong Chen(陈振东), Si-cong Liu(刘思聪), Xi Wang(王茜), Jiang Wang(王江), Yong-fang Li(李永放)
Chin. Phys. B . 2018, 27(11): 114214 . **doi:** 10.1088/1674-1056/27/11/114214

Diurnal cooling for continuous thermal sources under direct subtropical sunlight produced by quasi-Cantor structure

Jia-Ye Wu(吴嘉野), Yuan-Zhi Gong(龚远志), Pei-Ran Huang(黄培然), Gen-Jun Ma(马根骏), Qiao-Feng Dai(戴峭峰)
Chin. Phys. B . 2017, 26(10): 104201 . **doi:** 10.1088/1674-1056/26/10/104201

Absorption enhancement in thin film a-Si solar cells with double-sided SiO_2 particle layers

Chen Le, Wang Qing-Kang, Shen Xiang-Qian, Chen Wen, Huang Kun, Liu Dai-Ming
Chin. Phys. B . 2015, 24(10): 104201 . **doi:** 10.1088/1674-1056/24/10/104201

Giant transmission Goos–Hänchen shift in surface plasmon polaritons excitation and its physical origin

Yang Yang, Liu Ju, Li Zhi-Yuan
Chin. Phys. B . 2015, 24(7): 074201 . **doi:** 10.1088/1674-1056/24/7/074201

Influences of annealing temperature on properties of Fe^{2+}:ZnSe thin films deposited by electron beam evaporation and their applications to *Q*-switched fiber laser*

Du-Xin Qing(卿杜鑫)[1], Shu-Tong Wang(王树同)[1], Shou-Gui Ning(宁守贵)[1], Wei Zhang(张伟)[1], Xiao-Xu Chen(陈晓旭)[1], Hong Zhang(张弘)[1], Guo-Ying Feng(冯国英)[1,†], and Shou-Huan Zhou(周寿桓)[1,2]

[1] *Institute of Laser & Micro/Nano Engineering, College of Electronics & Information Engineering, Sichuan University, Chengdu* 610064, *China*
[2] *North China Research Institute of Electro-Optics, Beijing* 100015, *China*

(Received 31 January 2020; revised manuscript received 14 March 2020; accepted manuscript online 23 March 2020)

Fe^{2+}:ZnSe thin films are prepared on sapphire substrate at room temperature by electron beam evaporation and then annealed in vacuum (about 1×10^{-4} Pa) at different temperatures. The influences of thermal annealing on the structural and optical properties of these films such as grain size and optical transmittance are investigated. The x-ray diffraction patterns show that the Fe^{2+}:ZnSe thin film is preferred to be oriented along the (111) plane at different annealing temperatures. After the film is annealed, the full-width-at-half-maximum (FWHM) of the x-ray diffraction peak profile (111) of the film decreases and its crystal quality is improved. Scanning electron microscope images show that the films are more dense after being annealed. Finally, the sample is used as a saturable absorber in ZBLAN fiber laser. The annealed Fe^{2+}:ZnSe thin films can be used to realize stable *Q*-switching modulation on ZBLAN fiber laser. The results demonstrate that the Fe^{2+}:ZnSe thin film is a promising material for generating the high-power pulses of mid-infrared *Q*-switched fiber lasers.

Keywords: electron beam evaporation, thin film, optical materials, *Q*-switching

PACS: 42.60.Gd, 42.70.Hj **DOI:** 10.1088/1674-1056/ab81f2

1. Introduction

Transition metal (TM)-doped II–VI chalcogenides (such as Fe^{2+}:ZnSe and Cr^{2+}:ZnSe), as important mid-infrared laser materials, have the advantages of ultra-wideband gain, low saturation intensity, and large pump absorption coefficient.[1] They have aroused widespread interest in the scientific community.[2–7] Solid-state infrared lasers based on these materials reveal a wide tuning range, narrow linewidth, high energy, high output power, and high damage threshold.[1,7] The are widely used in biomedicine, laser spectroscopy, and space communications.[8–10] Among these materials, Fe^{2+}:ZnSe is an important mid-infrared material for the research of optoelectronic devices and lasers.[1,11] Fe^{2+}:ZnSe is not only a very excellent medium infrared laser material, but also an ideal passive saturable absorber.[12]

Typical saturable absorbers such as two-dimensional (2D) materials,[13–17] Cr^{4+}-doped crystals,[18,19] gold nanobipyramids (G-NBPs),[20] and Cr^{2+}-doped chalcogenide crystals[21] have been widely studied. As a saturable absorber, the working wavelength range of the Fe^{2+}:ZnSe laser is 2.5 μm–4.0 μm. Recently, the Fe^{2+}:ZnSe crystal saturable absorber (SA) for the passively *Q*-switching of fiber lasers has been reported to have working wavelengths around 3 μm[22] and 2.8 μm.[23] Furthermore the Fe^{2+}:ZnSe thin film for passively *Q*-switched fiber laser has been reported.[24,25] Compared with its bulk crystal SA, the Fe^{2+}:ZnSe thin film SA is easy to integrate on the optical element, resulting in a compact laser with fewer optical components. The properties of films are closely related to the methods by which they are prepared. The common preparation methods are electron beam evaporation,[26] pulsed laser deposited,[25] molecular beam epitaxy (MBE),[27,28] and chemical vapor deposition (CVD),[13] of which electron beam evaporation has the advantages of accurate electron beam positioning, fast evaporation rate, and less pollution. Annealing temperature is an important parameter for high-quality Fe^{2+}:ZnSe thin film prepared by electron beam evaporation at room temperature, which is used as an SA. Thus, we study the properties of Fe^{2+}:ZnSe thin films at different annealing temperatures and the modulation of laser is taken as an element.

In this work, the Fe^{2+}:ZnSe thin films are fabricated by electron beam evaporation at room temperature and vacuum annealing is performed at different temperatures for 600 min. Through analyzing the x-ray diffraction (XRD), Raman spectrum, optical transmittance, scanning electron microscope (SEM) micrographs, the structural and optical properties before and after the annealing treatment are studied, which can be used to compact the mid-infrared *Q*-switched fiber lasers, since these parameters play an important role in selecting laser

*Project supported by the National Natural Science Foundation of China (Grant No. 11574221) and the Graduate Student's Research and Innovation Fund of Sichuan University, China (Grant No. 2018YJSY008).

†Corresponding author. E-mail: guoing_feng@scu.edu.cn

© 2020 Chinese Physical Society and IOP Publishing Ltd

materials.

2. Experiment

The Fe^{2+}:ZnSe thin films were deposited on sapphire substrates by an electron beam evaporation system. The sapphire substrate (20 mm in diameter) is thoroughly washed with a plasma cleaner. The ZnSe and Fe powder (high purity, 99.99%, Sigma–Aldrich Co., Ltd.), placed in two separated crucibles, was used as an evaporation source in our method. The chamber pressure was kept as high as 4×10^{-4} Pa and substrate temperature was at room temperature. Deposition rate and film thickness were maintained and monitored using SQC-310 rate controller (INFICON) and a quartz crystal monitor.

The Fe^{2+}:ZnSe thin films were annealed in vacuum (about 1×10^{-4} Pa) at temperatures ranging from 100 ℃ to 400 ℃ for 600 min. The morphologies and structures of these films were determined by SEM, XRD, and Raman spectra. The optical transmissions of these films in a wavelength range of 1000 nm–5000 nm were measured by Fourier transform infrared spectrometer (Bruker, Tensor27), and the films were also employed in Q-switched fiber lasers. Finally, the thin film with good performance (400 ℃) was used for implementing the Q-switched modulation on a ZBLAN fiber laser.

3. Results and discussion

3.1. SEM results

The SEM is utilized for studying the surface morphologies of Fe^{2+}:ZnSe thin films annealed at different temperatures. Figure 1 shows the SEM images of as-deposited and annealed films at 100 ℃, 200 ℃, 300 ℃, 400 ℃ respectively. It can be seen that the cracks and pinholes are present on the as deposited film. However, after being annealed, the films seem to be more dense, cracks and pinholes gradually disappear. It may be due to the fact that the irregular and angular structures of these films have changed into round structures after being annealed and the annealed sample grains are merged with each other.[29] In addition, some small variations in particle size observed in SEM images show different quality of crystals at different annealing temperatures.[30]

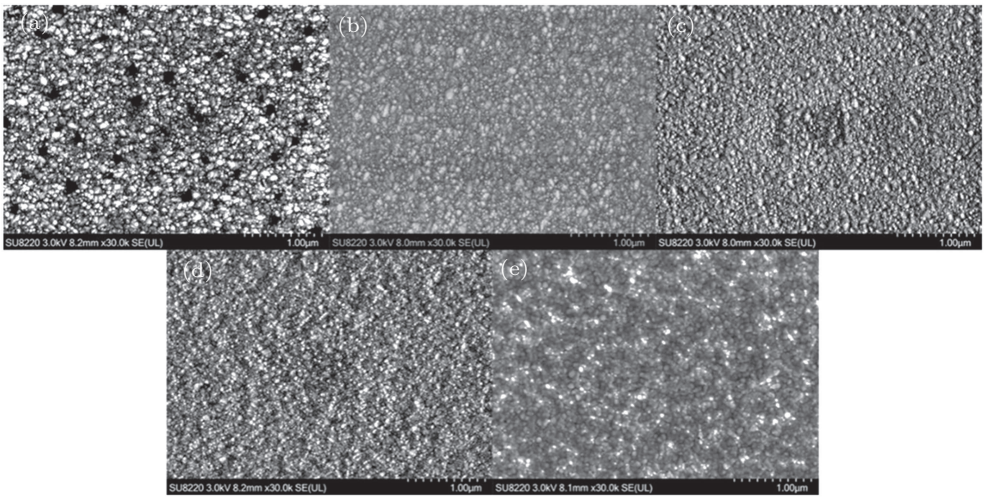


Fig. 1. Surface SEM images of Fe^{2+}:ZnSe films (a) as-deposited and annealed at (b) 100 ℃, (c) 200 ℃, (d) 300 ℃, and (e) 400 ℃.

3.2. X-ray diffraction analysis

The x-ray diffractions of as-deposited and annealed Fe^{2+}:ZnSe thin films are studied. The XRD patterns are shown in Fig. 2(a). It can be found that all the prominent peaks, along with the (1 1 1), (2 2 0), and (3 1 1) planes of polycrystalline Fe^{2+}:ZnSe, can be indexed as cubic sphalerite structure. It can be seen that 'as-deposited' Fe^{2+}:ZnSe thin film has a lower intensity reflection peak (1 1 1). The intensity of the (1 1 1) peak increases with annealing temperature increasing and becomes dominant at 200 ℃. This may be due to the rearrangement of atoms, the enhancement of clusters and the elimination of residual stresses/defects formed during the deposition of the film.[31] Beyond 200 ℃, this might be due to partial decomposition from the film surface, resulting in the decrease in intensity.[32,33] The grain sizes in the Fe^{2+}:ZnSe thin films annealed at different temperatures are also studied. The grain size of Fe^{2+}:ZnSe thin films can be calculated from the Scheler formula[32]

$$D = K\lambda/\beta\cos\theta. \tag{1}$$

The lattice parameter a is calculated from

$$a = d(h^2 + k^2 + l^2)^{1/2}, \tag{2}$$

where, l, k, and h represent the lattice planes.

The lattice spacing d is determined from the following Bragg's formula:

$$d = \lambda/2\sin\theta. \tag{3}$$

The microstrain (ε) value is calculated from

$$\varepsilon = \beta \cos\theta/4. \tag{4}$$

The dislocation density is calculated according to the following relation:[34]

$$\delta = 15\beta \cos\theta/4aD. \tag{5}$$

Here, λ is the wavelength of x-ray radiation, β is the full width at half maximum (FWHM) of XRD peak profile, θ is the Bragg diffraction angle of the XRD peak, and D is the grain size. The various structural parameters in Fe^{2+}:ZnSe thin films annealed at different temperatures are shown in Table 1, the lattice constants of the films deviate from the lattice constants of the bulk. This indicates that the crystallites of the film are formed under strain, which may be due to the changes in concentration and natural defects.[35] The grain size, strain, and dislocation density of the film are changed, and the effect of the film is better when the annealing temperature is 400 ℃. These observations could be explained by the fact that the film possesses higher adatom mobility and lower lattice defect concentration after it has been annealed, which results in the larger crystallite size and reduces the strain and dislocation density of the film.[29,36]

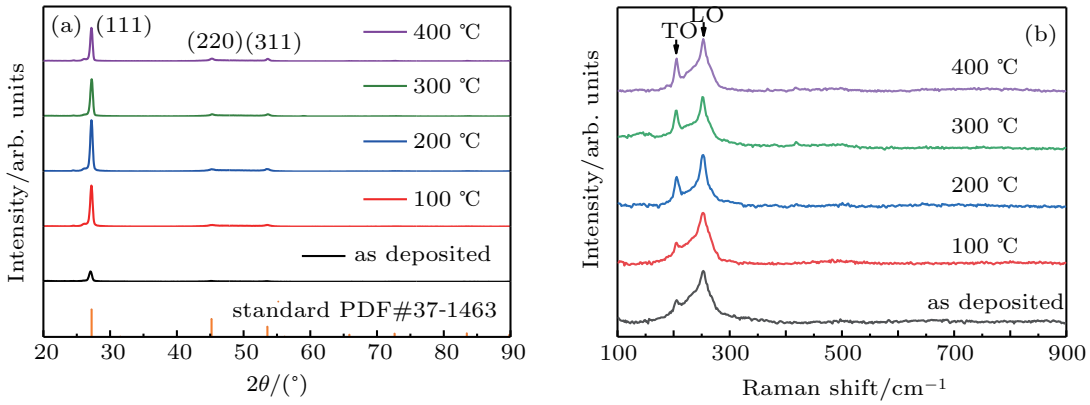


Fig. 2. (a) XRD patterns and (b) Raman spectra of Fe^{2+}:ZnSe films annealed at different temperatures.

Table 1. Structural parameters for (111) peak of Fe^{2+}:ZnSe films annealed at various temperatures.

Annealing temperature/℃	2θ/(°)	a/Å	d/Å	Grain size τ/nm	Strain $\times 10^{-3}\varepsilon$/(lin^{-2}·m^{-4})	Dislocation density $\times 10^{15}\delta$/(lin·m^{-2})
25 (as deposited)	27.042	5.7065	3.2947	17.42	1.99	3.00
100	27.2	5.6740	3.2759	19.05	1.82	2.52
200	27.201	5.6738	3.2758	19.32	1.79	2.45
300	27.239	5.6660	3.2713	19.10	1.81	2.52
400	27.2	5.6740	3.2759	20.48	1.69	2.18

3.3. Raman analysis

The Raman spectra for Fe^{2+}:ZnSe thin films at different annealed temperatures are shown in Fig. 2(b). The Raman measurement results are consistent with XRD analyses, indicating that the crystal quality of the film is better after being annealed. The well-resolved intense peaks at ~ 205 cm^{-1} and ~ 250 cm^{-1} are attributed to the transversal optical (TO) mode and longitudinal optical (LO) phonon mode of ZnSe, respectively,[37] indicating that ZnSe lattice has a high crystal quality.

3.4. Optical transmission

The information about optical transmittance is of great significance for assessing the optical properties of Fe^{2+}:ZnSe thin film. The transmission spectra of the Fe^{2+}:ZnSe thin film in a wavelength range of 1000 nm–5000 nm at different annealing temperatures are drawn in Fig. 3, it is shown that with the increasing of annealing temperatures, the absorption near 3-μm becomes more obvious. This is due to 3-μm centered absorption of Fe^{2+} instead of Zn^{2+} in ZnSe hosts.[24]

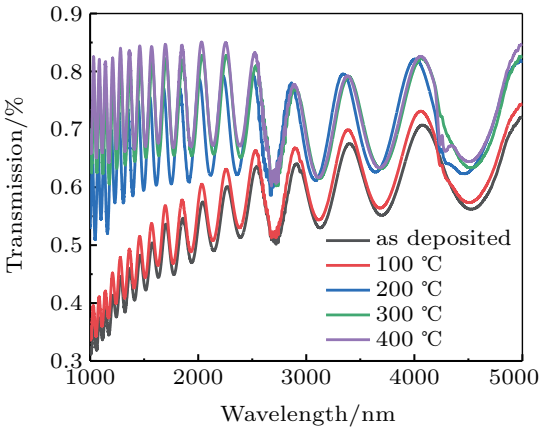


Fig. 3. Variations of transmission with wavelength of Fe^{2+}:ZnSe films annealed at various temperatures.

Based on the crystal field theory, the tetrahedral crystal field of the ZnSe host splits the ground level ^{5}D of Fe^{2+} into ^{5}E ground state and $^5T_2$ excited state, which have 5 and 6 spin–orbit levels respectively. Transitions between ^{5}E and $^5T_2$ are allowed, and in the Fe^{2+}:ZnSe system, it is expected that there will be multiple absorption lines between ~ 2 μm and ~ 4 μm and the absorption peak is located at ~ 3 μm.[7,27]

3.5. Application to *Q*-switched laser

The Fe^{2+}:ZnSe thin film annealed at 400 ℃ is used for implementing the *Q*-switched modulation on a ZBLAN fiber laser in Fig. 4. Figures 5(a)–5(c) show a typical passively *Q*-switched pulse string and the distribution of individual pulses at different pump powers. When the pump power is 1.251 W, a stable *Q*-switched pulse waveform is observed for the first time, and the average output power is 72 mW. In a typical passively *Q*-switched fiber laser, as the pump power increases, the average output power and repetition rate increase, and the pulse width decreases.[38] When the pump power is 8.27 W, a stable *Q*-switched pulse with a minimum pulse width of 0.618 μs, a repetition rate of 110.79 kHz, and an average output power of 660 mW is obtained. As can be seen from Fig. 5(d), the average output power increases from 72 mW to 660 mW as the pump power increases. Further increasing pump power, the *Q*-switched pulse turns unstable.

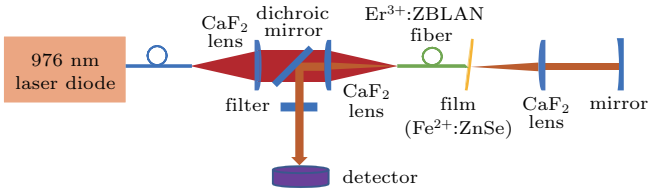


Fig. 4. Schematic diagram of passively *Q*-switched ZBLAN laser based on Fe^{2+}:ZnSe film.

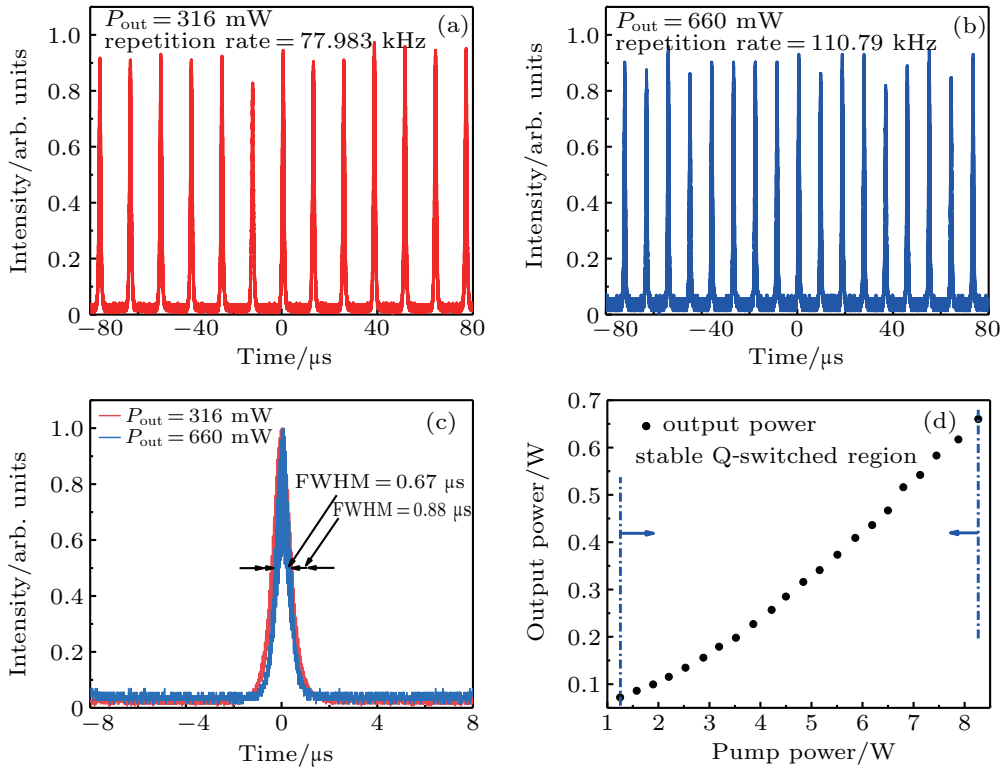


Fig. 5. Typical *Q*-switched pulse trains at output power of (a) 316 mW, (b) 660 mW, (c) single pulse waveform, and (d) average output power varying with pump powers.

In order to observe the stability of Fe^{2+}:ZnSe film *Q*-switched fiber laser, the RF output spectrum of *Q*-switched fiber laser with average output power of 660 mW is measured with an oscilloscope. As shown in Fig. 6(a), the signal-to-noise ratio of the spectrum is 43 dB, with a peak value of 110.78 kHz. It is slightly larger than some other Fe^{2+}:ZnSe passively *Q*-switched fiber lasers.[25,39] This fluctuation may be due to the thermal effect of Fe^{2+}:ZnSe.[40] In addition, the broadband RF spectrum is shown in Fig. 6(b).

The pulse duration and repetition rate of the Fe^{2+}:ZnSe thin film based *Q*-switched fiber laser *versus* pump power are shown in Fig. 7(a). The pulse width decreases from 1.776 μs to 0.618 μs as the incident pump power increases from 1.251 W to 8.27 W. The peak power and single-pulse energy *versus* pump power are shown in Fig. 7(b). The peak power and pulse energy of the stable *Q*-switched ZBLAN fiber laser increase with the pumping power increasing. The maximum single pulse energy is 5.96 μJ, which corresponds to a repetition rate of 110.79 kHz and the peak power of 9.64 W.

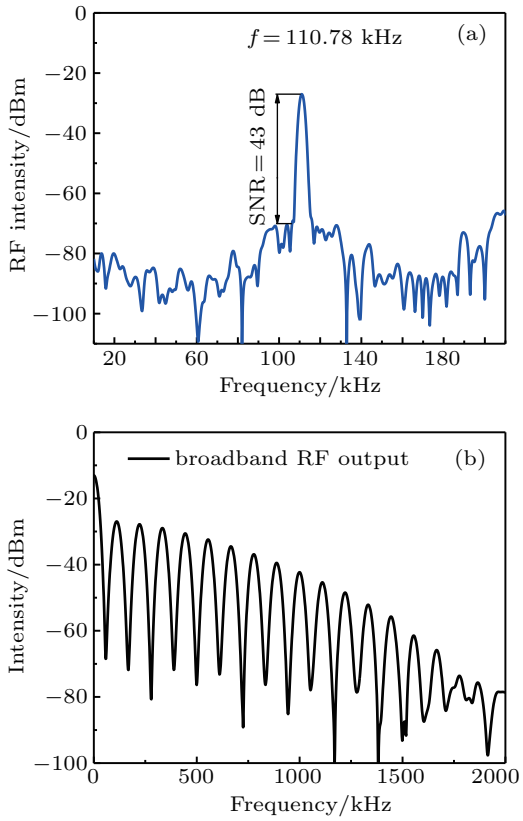


Fig. 6. (a) RF output spectrum of *Q*-switched fiber laser, and (b) broadband RF output.

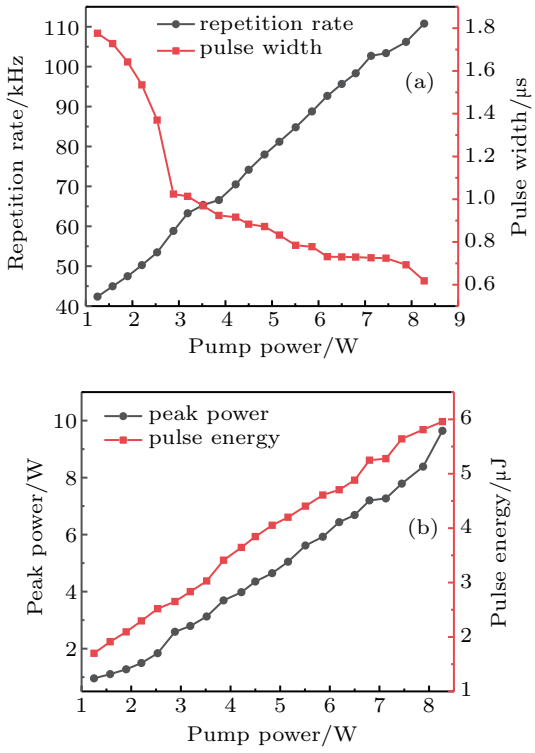


Fig. 7. (a) Repetition rate and pulse duration *versus* pump power, and (b) peak power and single-pulse energy *versus* pump power.

4. Conclusions

The Fe^{2+}:ZnSe thin films are prepared by the electron beam evaporation at an ambient temperature and annealed at different temperatures in vacuum for 600 min, and the effects of annealing treatment on structure, optical properties, and modulation properties are investigated. The XRD analyses and Raman spectra show that the annealing treatment can improve the crystallization performance of Fe^{2+}:ZnSe thin film. The SEM images show that the surface of the film is smoother and denser after being annealed. Annealing temperature plays an important role in controlling modulation parameters, structural and optical properties. The annealed Fe^{2+}:ZnSe thin films, used as a saturable absorber, can realize stable *Q*-switching modulation on ZBLAN fiber laser. The Fe^{2+}:ZnSe thin film is a promising material for generating the high-power pulses of mid-infrared *Q*-switched fiber lasers.

References

[1] Mirov S B, Fedorov V V, Martyshkin D, Moskalev I S, Mirov M and Vasilyev S 2015 *IEEE J. Sel. Topics Quantum Electron.* **21** 292
[2] Grebe G, Roussos G and Schulz H J 1976 *J. Lumin.* **12** 701
[3] DeLoach L D, Page R H, Wilke G D, Payne S A and Krupke W F 1996 *IEEE J. Quantum Electron.* **32** 885
[4] Lehr M U, Litzenburger B, Kreissl J, Pohl U, Selber H, Schulz H, Klimakow A and Worschech L 1997 *J. Phys.-Condes. Matter* **9** 753
[5] Page R H, Schaffers K I, DeLoach L D, Wilke G D, Patel F D, Tassano J B, Payne S A, Krupke W F, Chen K T and Burger A 1997 *IEEE J. Quantum Electron.* **33** 609
[6] Godlewski M, Surma M, Ivanov V Y and Surkova T 2004 *Low Temp. Phys.* **30** 891
[7] Mirov S B, Moskalev I S, Vasilyev S, Smolski V, Fedorov V V, Martyshkin D, Peppers J, Mirov M, Dergachev A and Gapontsev V 2018 *IEEE J. Sel. Topics Quantum Electron.* **24** 1
[8] Tittel F K 1998 *Appl. Phys. B* **67** 273
[9] Burger A, Chattopadhyay K, Ndap J O, Ma X, Morgan S, Rablau C, Su C H, Feth S, Page R H and Schaffers K I 2001 *J. Cryst. Growth* **225** 249
[10] Waynant R W, Ilev I K and Gannot I 2001 *Philos. Trans. R. Soc. London. Ser. A: Math. Phys. Eng. Sci.* **359** 635
[11] Mirov S B, Fedorov V, Martyshkin D, Moskalev I, Mirov M and Gapontsev V 2011 *Opt. Mater. Express* **1** 898
[12] Voronov A A, Kozlovskii V I, Korostelin Y V, Landman A I, Podmar'kov Y P, Polushkin V G and Frolov M P 2006 *Quantum Electron.* **36** 1
[13] Liu M L, OuYang Y Y, Hou H R, Lei M, Liu W J and Wei Z Y 2018 *Chin. Phys. B* **27** 084211
[14] Wang X, Li L, Li J P and Wang Y G 2017 *Chin. Phys. B* **26** 044203
[15] Sun Z, Cheng G H, Liu H, Wang X and Wang Y G 2017 *Chin. Phys. Lett.* **34** 014204
[16] Ling W, Xia T, Dong Z, Liu Q, Lu F and Wang Y 2017 *Acta Phys. Sin.* **66** 114207 (in Chinese)
[17] Hisamuddin N, Zakaria U, Zulkifli M, Latiff A, Ahmad H and Harun S 2016 *Chin. Phys. Lett.* **33** 074208
[18] Dun Y, Li P, Chen X and Ma B 2016 *Chin. Phys. Lett.* **33** 024201
[19] Liu Y, Liu Z, Cong Z, Xu X, Xu J, Men S, Xia J and Zhang S 2015 *Acta Phys. Sin.* **64** 174203 (in Chinese)
[20] Zhang F, Zhang H N, Liu D H, Liu J, Ma F K, Jiang D P, Pang S Y, Su L B and Xu J 2017 *Chin. Phys. B* **26** 024205
[21] Yang X T, Liu L and Xie W Q 2017 *Chin. Phys. Lett.* **34** 024201
[22] Li J, Luo H, Wang L, Zhai B, Li H and Liu Y 2015 *Opt. Express* **23** 22362
[23] Wei C, Zhu X, Norwood R A and Peyghambarian N 2012 *IEEE Photon. Technol. Lett.* **24** 1741
[24] Ning S, Feng G, Zhang H, Zhang W, Dai S and Zhou S 2019 *Opt. Mater.* **89** 473
[25] Zhang T, Feng G, Zhang H, Yang X, Dai S and Zhou S 2016 *Laser Phys. Lett.* **13** 075102
[26] Ning S, Feng G, Zhang H, Zhang W, Dai S, Xiao Y, Li W, Chen X and Zhou S 2018 *Opt. Mater. Express* **8** 865

[27] Polyakov S M, Karhu E, Zamiri R, Moisset C, Iliopoulos K, Vullum P E, Osterberg U L and Gibson U J 2018 *Opt. Mater. Express* **8** 356

[28] Tolstik N, Sorokin E, Karhu E A, Gorbachenya K, Polyakov S M, Kisel V E, Kuleshov N, Furtula V, Gibson U J and Sorokina I T 2018 *Opt. Mater. Express* **8** 522

[29] Bacaksiz E, Aksu S, Polat I, Yılmaz S and Altunbaş M 2009 *J. Alloys Compd.* **487** 280

[30] Ou K, Wang S, Huang M, Zhang Y, Wang Y, Duan X and Yi L 2018 *J. Lumin.* **199** 34

[31] Alam M J and Cameron D C 2000 *Thin Solid Films* **377–378** 455

[32] Bedir M, Öztaş M, Bakkaloğlu Ö and Ormanci R 2005 *Eur. Phys. J. B-Condens. Matter Complex Syst.* **45** 465

[33] Subbaiah Y V, Prathap P, Devika M and Reddy K R 2005 *Physica B* **365** 240

[34] De C and Misra N 1997 *Indian J. Phys.* **A71** 535

[35] Venkatachalam S, Mangalaraj D, Narayandass S K, Kim K and Yi J 2005 *Physica B* **358** 27

[36] Kalita P K, Sarma B and Das H 2000 *Bull. Mater. Sci.* **23** 313

[37] Williams J, Fedorov V, Martyshkin D, Moskalev I, Camata R and Mirov S 2010 *Opt. Express* **18** 25999

[38] Zhu G, Zhu X, Balakrishnan K, Norwood R A and Peyghambarian N 2013 *Opt. Mater. Express* **3** 1365

[39] Ning S, Feng G, Dai S, Zhang H, Zhang W, Deng L and Zhou S 2018 *AIP Adv.* **8** 025121

[40] Herda R, Kivistö S and Okhotnikov O G 2008 *Opt. Lett.* **33** 1011